Few-nucleon transfer in quasi-elastic collisions at 20 MeV/nucleon

H. Utsunomiya,* E. C. Deci,† R. A. Blue, L. H. Harwood, R. M. Ronningen,
K. Siwek-Wilczynska,‡ and J. Wilczynski§
National Superconducting Cyclotron Laboratory, Michigan State University, East Lansing, Michigan 48824

D. J. Morrissey
National Superconducting Cyclotron Laboratory and Department of Chemistry, Michigan State University, East Lansing, Michigan 48824

(Received 30 August 1985)

We report measurements of the isotopic distributions of targetlike fragments in coincidence with nitrogen, carbon, and boron isotopes from the reaction of 20 MeV/nucleon ^{14}N with ^{165}Ho and ^{164}Dy. The binary nature of the reaction was studied by observing particle-γ-ray coincidences; projectilelike fragments were identified near the classical grazing angle with a telescope consisting of silicon surface barrier detectors, and the targetlike fragments were identified by observing their discrete deexcitation γ rays in either of two high purity germanium detectors. The following reactions were studied: ^{164}Dy(^{14}N,χxn), ^{164}Dy(^{14}N,$\chi\alpha$xn), ^{165}Ho(^{14}N,Cχn), ^{165}Ho(^{14}N,C$\alpha\chi$n), where χ=nitrogen or boron isotopes. The inclusive energy spectra of the projectilelike fragments are reasonably described by either the extended Serber or the Friedman model of projectile breakup. Such interpretations of the reaction mechanism were further tested by comparing the targetlike fragment isotopic distributions to those expected from transfer of the unobserved breakup fragment to the target followed by statistical decay. The agreement of the predicted targetlike fragment isotopic distributions with the present data is remarkably good.

I. INTRODUCTION

At bombarding energies on the order of 10 MeV/nucleon, peripheral collisions of heavy ions with medium and large mass ($A \sim 150$–200) nuclei are well characterized by binary processes.[1–4] The observation of projectilelike fragments (PLF's) in such binary processes is coupled to the formation of a targetlike fragment (TLF) at an excitation energy and angular momentum corresponding to capture of the unobserved or missing mass. Such transfers between the colliding nuclei have been particularly well described by the sum-rule model of incomplete fusion reactions.[4] At higher bombarding energies, the description of the reaction in terms of projectile breakup in the vicinity of the target has been successfully applied.[5] Such breakup reactions can lead to "binary" processes when one of the projectile fragments is captured by the target; this is sometimes labeled "breakup fusion."[6] In addition, the target may fail to capture the fragment which leads to a ternary process.[5,7] As an added complication, we know that excited projectilelike fragments can sequentially decay in flight, another ternary process.[5,7]

Experimental investigation of the binary nature of a nuclear reaction requires either a complete measurement of all products or at least a technique that identifies the mass and charge of both reaction partners. The combination of a mass-asymmetric reaction system in which the light fragment is identified in a conventional telescope consisting of Si surface barrier detectors, with high resolution γ-ray spectroscopy identifying the targetlike fragments, adequately fulfills the requirements. The present paper reports measurements of the targetlike fragments (TLF's) observed in coincidence with quasi-elastic projectilelike fragments (PLF's) from the reaction of ^{14}N with ^{165}Ho and ^{164}Dy at 20 MeV/nucleon. The Ho and Dy were used so that transfer of one and two units of charge, respectively, would lead to well-characterized Er nuclei.

In this paper, we present exclusive cross sections for charge binary reactions determined from particle-(i.e., PLF)-γ-ray coincidence measurements as well as inclusive kinetic energy spectra of these projectilelike fragments. The shape of the kinetic energy spectra compares favorably with the predictions of the extended Serber model[8] and the Friedman model[9] of projectile breakup. The isotopic distributions of the TLF were compared to those expected for projectile breakup followed by capture of the unobserved fragment and sequential statistical decay of the newly excited TLF. These comparisons were surprisingly good, and lend support to the breakup models.

The details of the experiment are given in Sec. II, followed by the inclusive differential cross sections of the PLF and exclusive cross sections for the charge-binary reactions in Sec. III. In contrast to low energy heavy-ion reactions, at 20 MeV/nucleon the present particle-γ coincidence technique was found to be limited to studies of the transfer of one or two units of charge because the excitation energy of the heavy residues becomes so high that a broad range of final residues is produced. The data are interpreted in the framework of projectile breakup in Sec. IV. Concluding remarks are contained in Sec. V. A preliminary report of this work has appeared as Ref. 10.

II. EXPERIMENTAL

A beam of 20 MeV/nucleon ^{14}N ions was obtained from the K500 cyclotron of the National Superconducting Cyclotron Laboratory at Michigan State University. We used targets of 2.3 mg/cm^2 ^{165}Ho and 2.0 mg/cm^2 ^{164}Dy in order to produce even-Z targetlike residue nuclei (Dy and Er isotopes). The impurities in the ^{164}Dy target were measured with a 10 MeV α beam from the tandem Van de Graaff of the Western Michigan University. Elastic scattering indicated that the equivalent of 25 μg/cm^2 carbon and approximately 100 μg/cm^2 thorium (the reducing agent for dysprosium oxide) were present in the target. The heavy-ion beam was stopped in a heavily shielded Faraday cup located approximately 3 m downstream from the target; the Faraday cup was connected to a current digitizer which recorded the current as a function of time.

The PLF's were detected and the isotopes were clearly identified in a telescope consisting of 100 μm silicon ΔE of high planarity and 1 mm E detector. The telescope was located at 14° with respect to the beam (near the classical grazing angle) and was inclined by 30° out of the horizontal plane (such an inclination was important for obtaining the γ-ray angular anisotropy). The telescope had an opening angle of $\pm 3.5°$ and a solid angle of 12.6 msr. Isotope separation was maintained during the measurements by cooling the silicon detectors to -30°C. Complete energy spectra of PLF's with $5 \leq Z \leq 8$ were obtained, while fragments with $Z \leq 4$ punched through the E detector. The particle singles were prescaled by a factor of 32 and were written on magnetic tape along with all the particle-γ-ray coincidence events. The normalizations used to get absolute cross sections were obtained from the measured target thickness, the detector solid angle, and the beam current collected in the Faraday cup. The absolute uncertainty in the cross sections is estimated to be less than 20 percent, and is dominated by the effects of target nonuniformities.

Discrete γ-ray transitions from the heavy residues were observed with either of two high purity germanium (HPGe) detectors placed above the plane of the scattering chamber as indicated in Fig. 1. In addition, a set of four bismuth germanate detectors (BGO) were also placed above the plane of the scattering chamber in order to observe discrete γ-ray transitions from the PLF's. This facet of the experiment has been reported elsewhere.[11] The HPGe detectors had active volumes of 89 and 77 cm^3 and were placed approximately 16 and 13 cm from the target, respectively. The energy resolution of the HPGe detectors was about 1.9 keV at low counting rates and about 2.1 keV at counting rates of approximately 14000 counts/sec. Degradation of the energy resolution at these higher counting rates forced us to limit the beam intensity so that the HPGe counting rates remained at approximately 20000 counts/sec during the measurements. Coincidences between any PLF and a γ ray with an energy between 80 keV and 2 MeV triggered the electronic logic and were recorded on magnetic tape. The energy calibration and photopeak efficiency of each HPGe detector was measured with standard γ-ray sources. The coincidence efficiency of the entire setup was checked with

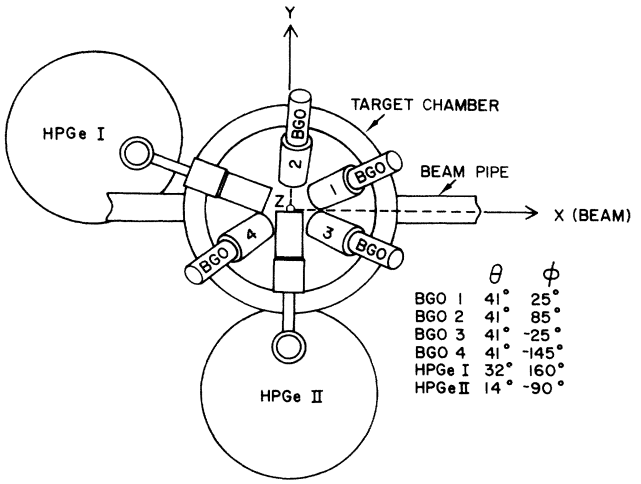

FIG. 1. Schematic diagram of the experimental apparatus (top view) with two high purity germanium detectors and four bismuth germanate detectors.

^{60}Co, ^{207}Bi, and ^{22}Na sources.

Coincidence cross sections for the charge-binary reactions were obtained according to a method described previously.[12] Briefly, the photopeak yields were corrected for losses due to electron conversion, differing branching ratios, angular anisotropies, and pileup in the spectroscopy amplifier. The 4^+-2^+ transition was used to determine the cross section for most even-even TLF's, unless the transition suffered from a neighboring unresolvable peak. In such cases the 6^+-4^+ transition was used. The branching ratio was assumed to be 1 for all of these transitions in the even-even TLF's. Note that the 2^+-0^+ transition was generally near the electronic threshold and was highly converted into electrons. For the odd mass TLF's, the following γ rays were used to calculate the cross section: 306.1 keV (^{165}Er: a doublet of $\frac{21}{2}^+ - \frac{17}{2}^+$ and $\frac{19}{2}^+ - \frac{15}{2}^+$), 217.6 keV ($^{163}Er$: $\frac{17}{2}^+ - \frac{13}{2}^+$), 198.6 keV ($^{161}Er$: $\frac{17}{2}^+ - \frac{13}{2}^+$), 167.3 keV ($^{163}Dy$: $\frac{9}{2}^- - \frac{5}{2}^-$), 167.0 keV ($^{161}Dy$: $\frac{13}{2}^+ - \frac{9}{2}^+$), and 177.6 keV ($^{159}Dy$: $\frac{5}{2}^+ - \frac{3}{2}^-$). Since the 198.6 keV γ ray of ^{161}Er was not resolved from the 4^+-2^+ transition of ^{160}Dy in the boron channels, the intensity of the 4^+-2^+ transition was estimated from the preceding 6^+-4^+ transition, assuming no side feeding. The branching ratio for each of these transitions was obtained from previous in-beam γ-ray spectroscopic data.[13] The angular anisotropies were estimated by comparison of the yields obtained from the two HPGe detectors. The pileup probability, for which a correction was not made in a preliminary report,[10] was fairly large in our experimental arrangement. We measured the pileup probability off line as a function of γ-ray counting rates. Taking into account the beam instability during the experiment, the photopeak yield was estimated to be reduced to 43 ± 9% at an amplifier shaping time of 3 μsec.

Four 7.6 cm$\times$7.6 cm bismuth germanate detectors were placed at 17.5 cm from the target, each pointing at the target with an angle of 49° with respect to the horizontal plane (see Fig. 1). These detectors were used to identi-

fy discrete transitions from the PLF and had fairly high γ-ray energy thresholds (approximately 350 to 400 keV). The events with coincidences between a BGO and a PLF detector were also recorded on magnetic tape.

III. RESULTS

We summarize the energy integrated cross sections of PLF's in Table I. The inclusive energy spectra of products from the reaction of $^{14}N + {}^{165}Ho$ are shown in Figs. 2–4. The energy spectra have a familiar shape with large cross sections centered at an energy approximately corresponding to the beam velocity and with tails extending toward large negative Q values. The energy spectra predicted by the projectile breakup models, discussed below, are also shown in Figs. 2–4. The gaps in the data are regions contaminated by pileup and other secondary effects associated with the very intense elastic scattering peak.

TABLE I. Inclusive cross sections of projectilelike fragments in mb/sr.

Ejectile	$d\sigma/d\Omega$ ($\theta_{lab}=14°$)[a]	
	^{164}Dy	^{165}Ho
^{16}O	5.5	5.8
^{15}O	9.7	14.
^{15}N	160.	217.
^{13}N	51.	95.
^{14}C	21.	27.
^{13}C	109.	157.
^{12}C	230.	319.
^{11}C	25.	35.
^{13}B	4.2	4.9
^{12}B	16.	21.
^{11}B	114.	146.
^{10}B	54.	67.

[a]The estimated uncertainties are 20 percent; see the text.

The primary goal of the present experiment was to identify the targetlike fragments in coincidence with the readily observable projectilelike fragments. This involves identification of known transitions in the discrete γ-ray

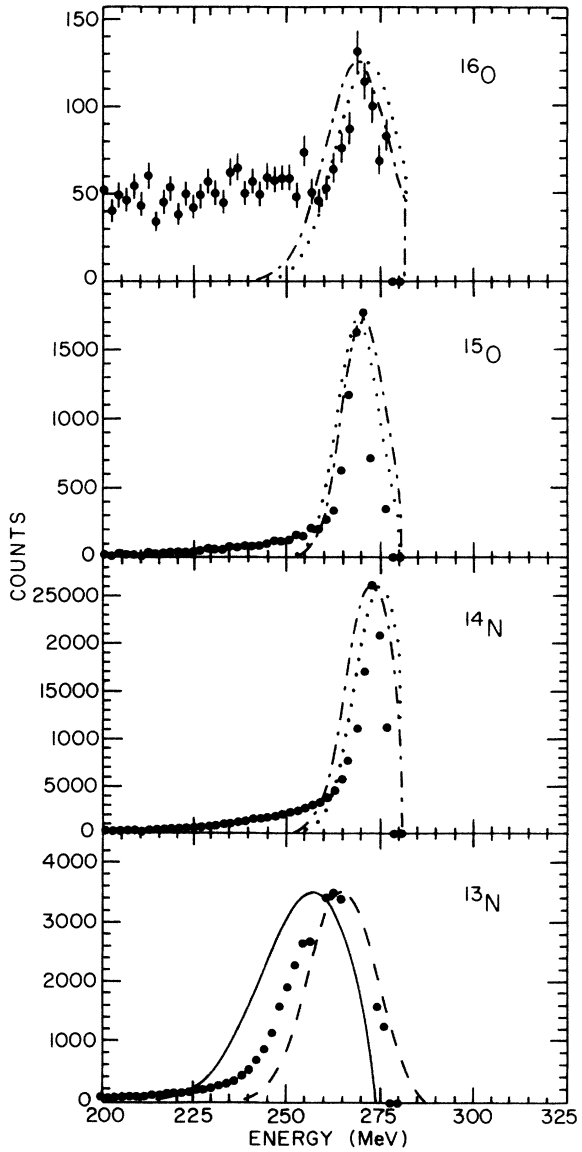

FIG. 2. Inclusive spectra of ^{16}O, ^{15}O, ^{15}N, and ^{13}N fragments from the $^{14}N + {}^{165}Ho$ reaction at 20 MeV/nucleon. The dotted and the dotted-dashed curves are the results of the pickup model calculations with two sets of parameters (see the text). The solid and dashed curves are the results of the Friedman model and the extended Serber model calculations, respectively. The arrows indicate the energies corresponding to the beam velocity.

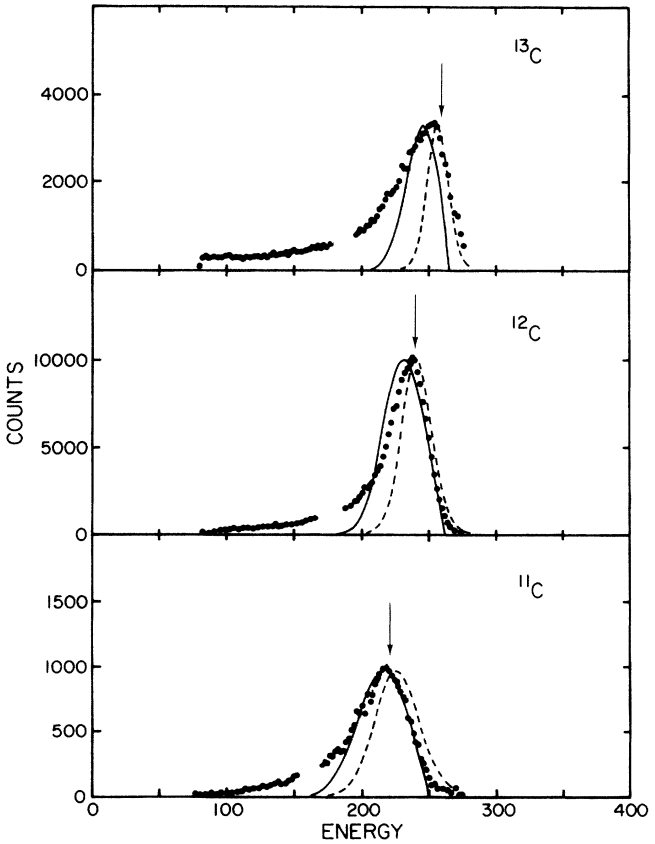

FIG. 3. Inclusive spectra of ^{13}C, ^{12}C, and ^{11}C, similar to Fig. 2.

TABLE II. Coincidence cross sections of targetlike fragments in mb/sr.

Target	Ejectile	$d\sigma/d\Omega$ ($\theta=14°$) (mb/sr) 0n	1n	2n	3n	4n	5n	6n	7n	8n
^{164}Dy	^{15}N		3.4±0.5	2.3±0.4	0.8±0.3					
	^{13}N	2.4±0.3		1.2±0.2						
^{164}Dy	^{12}B			0.2±0.1	0.4±0.2	0.4±0.1	<0.6	0.2±0.1		
	^{11}B			0.6±0.4	1.4±0.4	2.2±0.6	1.5±0.4	1.5±0.8	1.4±0.4	
	^{10}B				0.5±0.3	1.0±0.3	1.3±0.5	0.7±0.2	<1.1	0.6±0.3
^{165}Ho	^{13}C		1.2±0.7	2.2±0.6	1.5±0.8	1.7±0.6				
	^{12}C		1.9±0.8	3.5±1.2	7.3±1.2	3.0±1.7	2.3±0.9	1.6±0.5	<1.3	
	^{11}C			<0.4	<0.8	0.8±0.3	0.7±0.4	<0.5	0.5±0.3	<0.4
		α0n	α1n	α2n	α3n	α4n	α5n	α6n		
^{164}Dy	^{12}B		0.2±0.1	<0.4	0.2±0.1					
	^{11}B			0.7±0.3	0.6±0.4	<0.9	<0.7			
	^{10}B			0.4±0.2	0.5±0.3	<0.7	<0.9	0.5±0.2		
^{165}Ho	^{13}C	0.8±0.4	<0.8							
	^{12}C		1.0±0.7	1.3±0.6	1.0±0.6	<1.3				
	^{11}C				<0.5	<0.7	<0.3			

spectra taken with the HPGe detectors in coincidence with each PLF. Figures 5, 6, and 7 show these coincidence spectra for the series of nitrogen, carbon, and boron isotopes, respectively. The transitions from the dominant reaction channels of neutron evaporation, xn, and rather weak channels of alpha plus neutron evaporation,

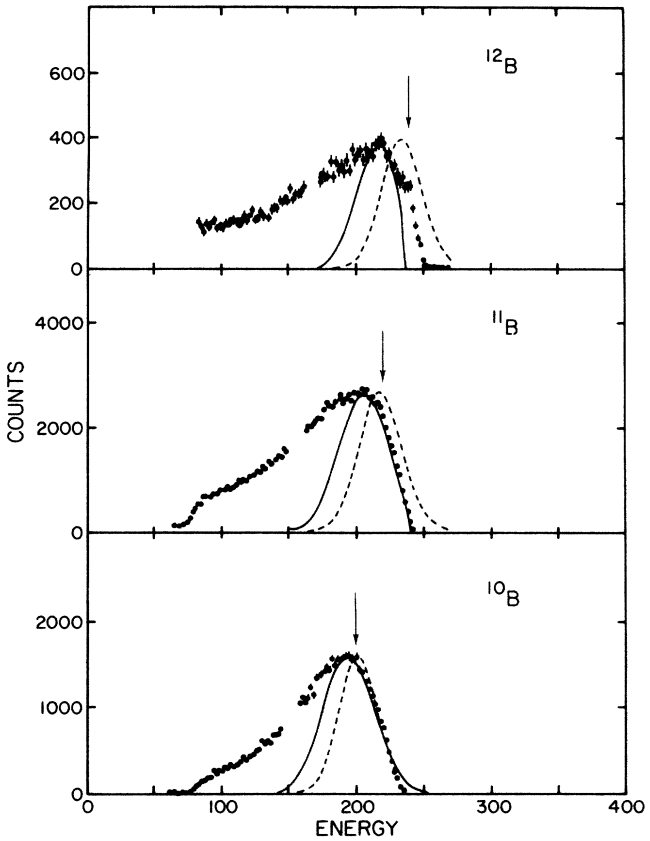

FIG. 4. Inclusive spectra of ^{12}B, ^{11}B, and ^{10}B, similar to Figs. 2 and 3.

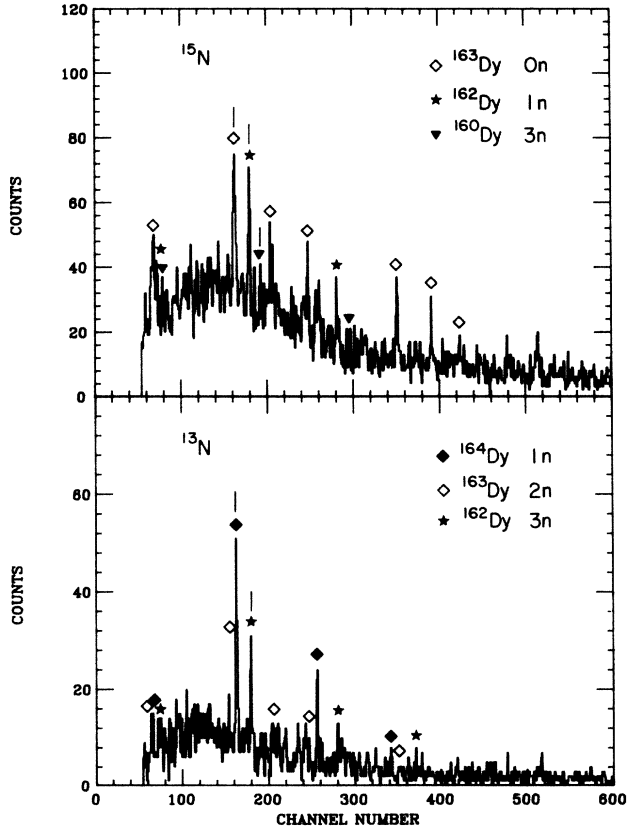

FIG. 5. Discrete γ-ray spectra from a HPGe detector in coincidence with ^{15}N and ^{13}N from the reaction of ^{14}N + ^{164}Dy at 20 MeV/nucleon. Channel numbers approximately correspond to keV. Each symbol uniquely represents one isotope in the three panels of the figure. Some of the γ-ray transitions used to obtain cross sections are marked with the bars, as discussed in the text.

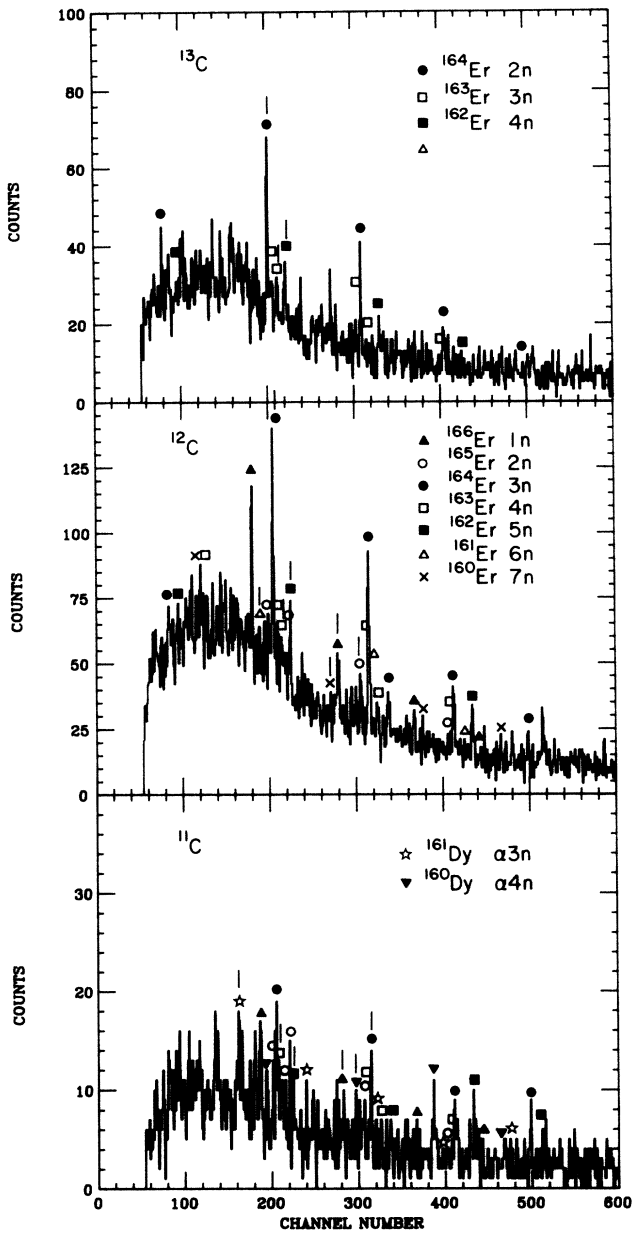

FIG. 6. Discrete γ-ray spectra from a HPGe detector in coincidence with ^{13}C, ^{12}C, and ^{11}C from the reaction of ^{14}N + ^{165}Ho at 20 MeV/nucleon, similar to Fig. 5.

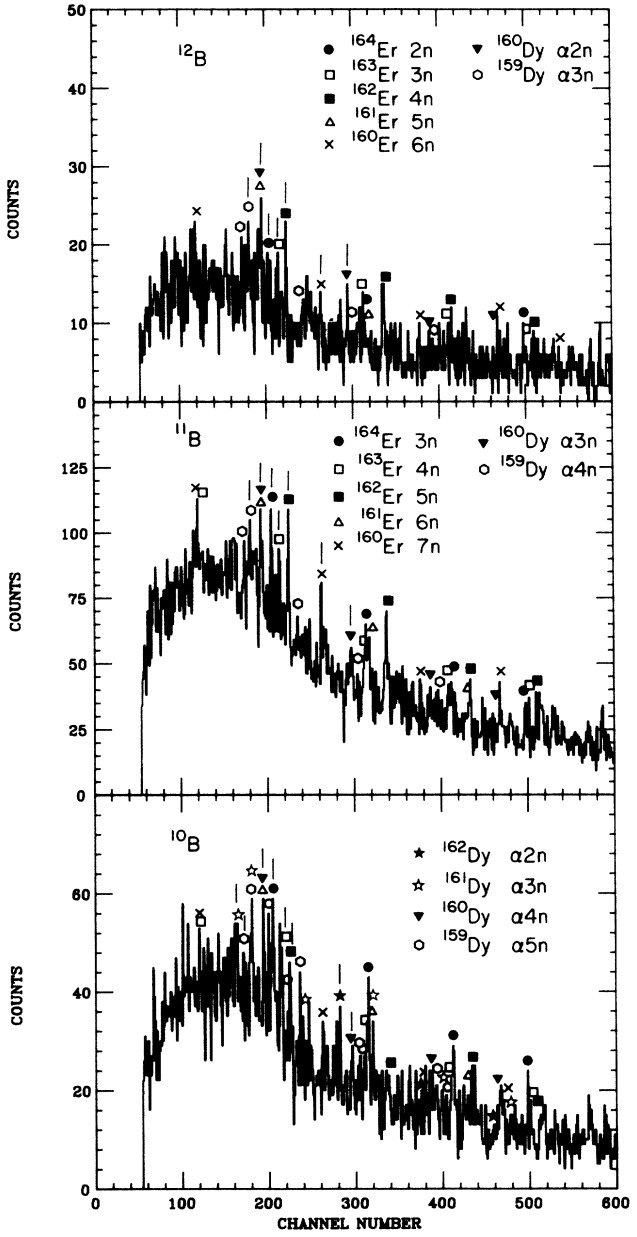

FIG. 7. Discrete γ-ray spectra from a HPGe detector in coincidence with ^{12}B, ^{11}B, and ^{10}B from the reaction of ^{14}N + ^{164}Dy at 20 MeV/nucleon, similar to Figs. 5 and 6.

αxn, are indicated in the figures. In general, these figures show that as the mass number of the PLF decreases, the number of missing neutrons increases, as expected in a binary process in which an unobserved projectilelike fragment is absorbed by the target. However, this is not true for the αxn channels, which most likely occur via the α-particle breakup of primary PLF's accompanied by mutual excitation of the targetlike residue. It is also noted that the ratio of the observable discrete γ rays to background (continuum γ rays) becomes poor and the number of reaction subchannels increases with decreasing mass number of PLF. This aspect limited the present study of binary reactions to measurements of the transfer of one or two units of charge. Future studies using Compton-suppressed germanium detectors should be able to extend the measurements to larger charge (mass) transfer.

In Table II, we summarize the cross sections for the observed subchannels. The ratios of the exclusive cross sections, integrated over various subchannels, to the corresponding inclusive cross sections are listed in Table III. Notice that small fractions, in the range of 4 to 10 percent, of the inclusive cross sections for nitrogen, carbon, and boron isotopes are associated with "binary" reactions. These fractions are considerably smaller than those observed by Wald *et al.*[17] in a charged particle coincidence measurement; this may be due to the impurities in our target.

TABLE III. Summed targetlike fragment cross sections.

Reaction	$d\sigma/d\Omega$ ($\theta=14°$)[a] (mb/sr)	Fractions (percent)
	(a) ^{164}Dy target	
^{164}Dy(^{14}N,^{15}Nxn)	7 ±2	4±1
^{164}Dy(^{14}N,^{13}Nxn)	4 ±1	8±2
^{164}Dy(^{14}N,^{12}Bxn)	1.4±0.9	9±6
(^{14}N,^{12}Bαxn)	<1	<6
^{164}Dy(^{14}N,^{11}Bxn)	9 ±3	8±3
(^{14}N,^{11}Bαxn)	2 ±1	2±1
^{164}Dy(^{14}N,^{10}Bxn)	5 ±2	9±4
(^{14}N,^{10}Bαxn)	2 ±1	4±2
	(b) ^{165}Ho target	
^{165}Ho(^{14}N,^{13}Cxn)	7 ±3	4±2
(^{14}N,^{13}Cαxn)	<2	<1.3
^{165}Ho(^{14}N,^{12}Cxn)	20 ±7	6±2
(^{14}N,^{12}Cαxn)	4 ±2	1±0.6
^{165}Ho(^{14}N,^{11}Cxn)	3 ±2	9±6
(^{14}N,^{11}Cαxn)	<1.5	<4.2

[a]Uncertainties represent any statistical errors. The uncertainties in the absolute cross sections due to the nonuniformity of the target and the pileup probability (see the text) are less than 20%.

IV. DISCUSSION

A. Inclusive energy spectra

Several models of projectile breakup have been suggested that describe the final momentum of PLF's *lighter* than the projectile in terms of two components, the fragment's fraction of the initial beam momentum and the momentum due to internal motion prior to breakup (e.g., Refs. 8 and 9 and references therein). It is this internal momentum distribution that gives rise to the broad energy peaks observed for PLF's. A detailed discussion of the energy spectra of PLF's *heavier* than the projectile is presented in the Appendix as it is not the main subject of this paper.

We applied the Friedman model to the data of the inclusive PLF spectra by taking into account the following aspects of the reaction: (i) the breakup of the projectile into its constituent clusters was assumed to take place at the nuclear surface of the target, (ii) the projectile was decelerated in the Coulomb field of the entrance channel and the ejectile was accelerated in the exit channel, and (iii) a three-body phase space factor,[14] $\rho=A_1P_1A_2P_2$ where A_1 and A_2 denote the mass numbers of the ejectile and the unobserved fragment and P_1 and P_2 stand for their momenta, respectively, was employed. Inclusion of the three-body phase space factor seems reasonable for inclusive spectra because, as shown in Sec. III, binary processes are less important at this bombarding energy. Throughout the entire process, we assumed that the projectile and the ejectile follow classical grazing trajectories. Because the angular acceptance of the telescope was large, ±3.5° at an average angle of 14°, the final momenta of the ejectiles were weighted according to classical Coulomb (Rutherford) angular distribution. Such a steep angular distribution is consistent with the experimental data for quasi-elastic scattering at 20 MeV/nucleon.[15] The free parameters in this model are the truncation radius for the internal wave function of the projectile fragments, the separation of the target and beam nuclei at breakup, plus an individual normalization. We used a truncation radius of $1.2A_1^{1/3}$ fm, as determined in a previous study,[9] and a breakup radius of $1.4(A_p^{1/3}+A_t^{1/3})$ fm with the mass numbers of the projectile (A_p) and the target (A_t). The results of the calculation were insensitive to the value of the radius parameter over a range of 50 percent. The solid curves in Figs. 2—4 show the results of these calculations.

We also applied the extended Serber model[8] to the same data. In this model it is assumed that one of the constituent clusters in the projectile misses the target and continues its flight as a spectator, while the other cluster strikes the target and undergoes a strong interaction with the target. The phase space factor is simply given by A_1P_1 because the fate (either absorption or scattering) of the unobserved fragment is not specified in this model. Aspect (ii) of the reaction discussed above was taken into account by replacing the beam and ejectile momenta with their local momenta just before and after the breakup, respectively, as has been done in Ref. 8. The results are shown by the dashed line in Figs. 2—4.

The peak positions of the Friedman model calculations (solid curves) are slightly shifted toward lower energy compared to those of the extended Serber model calculations (dashed curves). This is due to the kinematics employed in the Friedman model, where a small portion of the bombarding energy is first used to break up the projectile. Note that in the extended Serber model, the most probable velocity of the ejectile nearly equals the beam velocity because of the spectator approximation for the ejectile. The three-body phase space factor used in the Friedman model results in a rapid decline of the spectra on the higher energy side, while the extended Serber model predicts nearly symmetric spectra. Overall, both calculations reproduce the experimental data acceptably well.

B. Exclusive reactions

Table III summarizes the cross sections for the production of targetlike residues in coincidence with specific PLF's along with their fractions of the inclusive PLF cross sections. It should be stated that the missing neutrons in the PLF, xn channels are most likely evaporative, while the missing α particle in the PLF, αxn channels seems nonevaporative. For the former case we reproduce the neutron distributions on the basis of the statistical evaporation model assuming that the unobserved frag-

ment is absorbed by the target, as discussed below. In such a statistical evaporation framework, evaporative α cross sections are found to be less than 1% of evaporation neutron cross sections for the present cases. Therefore, it is more likely that the observed γ-αxn events correspond to sequential decay[5,7] of primary PLF's in those particular reactions in which the target is simultaneously excited. Consequently, the heavy ion (HI), αxn cross sections given in Table III should be regarded as upper limits to the cross section for such mutual excitation processes. Thus, we regard only the xn cross sections as the binary cross sections. Our results indicate that a binary reaction partner was observed in coincidence with only 4 to 10 percent of the PLF's.

The most important aspect of the present study is the correlation of the PLF's with targetlike residues. We can make a more stringent test of the projectile breakup mechanism described above by comparing the observed TLF mass distributions with model predictions. However, in order to make such a comparison we again need to extend the breakup model. A capture of the unobserved part of the projectile by the target will create a targetlike nucleus at a specific excitation energy and angular momentum which can be coupled to the calculated kinetic energy distribution of the observed PLF. Thus, we can convert the kinetic energy distribution predicted for a specific PLF into an excitation energy distribution of a specific targetlike fragment and then follow its evaporation statistical equilibrium decay.

The kinetic energy distributions from the Friedman model were used to calculate the excitation and angular momentum distributions of the primary TLF's. The peaks shown in Figs. 2–4 were divided into eight energy bins. A targetlike compound nucleus was assumed to be produced by the absorption of the unobserved projectile fragment corresponding to each bin. The beam nucleus delivers the fragment of the target nucleus at the top of the Coulomb barrier and thus the excitation energy of the primary TLF is taken to be the sum of the transferred fragment's kinetic energy and the Q value for the capture reaction leading to the formation of the compound nucleus. For the present simple estimates we assume an opaque target nucleus; that is the probability of the absorption of the unobserved fragment is independent of its kinetic energy and direction of incidence on the target. This is clearly a limiting case for the model and so we will only consider the variation of the relative yields of the TLF isotopes.

The statistical decay of the targetlike compound nuclei was followed with the ORNL-ALICE computer code.[16] This code predicts that either one or two evaporated residues will be produced for a given energy bin (see Fig. 8). However, the momentum distribution of the absorbed fragments produce a distribution of excitation energies and angular momenta. The range of these excitation energies and angular momenta is indicated in Table IV. The evaporation residues from the eight compound nuclei decay chains were then weighted in proportion to the PLF kinetic energy distribution and added together.

The relative isotopic distributions are compared to the data in Fig. 9. In most cases the fits are unexpectedly

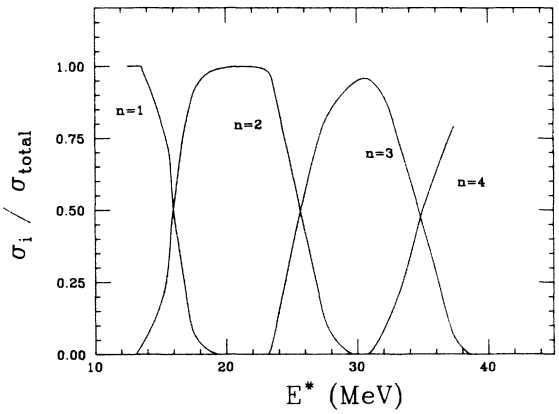

FIG. 8. Calculated ratios of cross sections for a given neutron multiplicity to the total cross section for particle emission versus excitation energy of the equilibrated compound nucleus ^{166}Er.

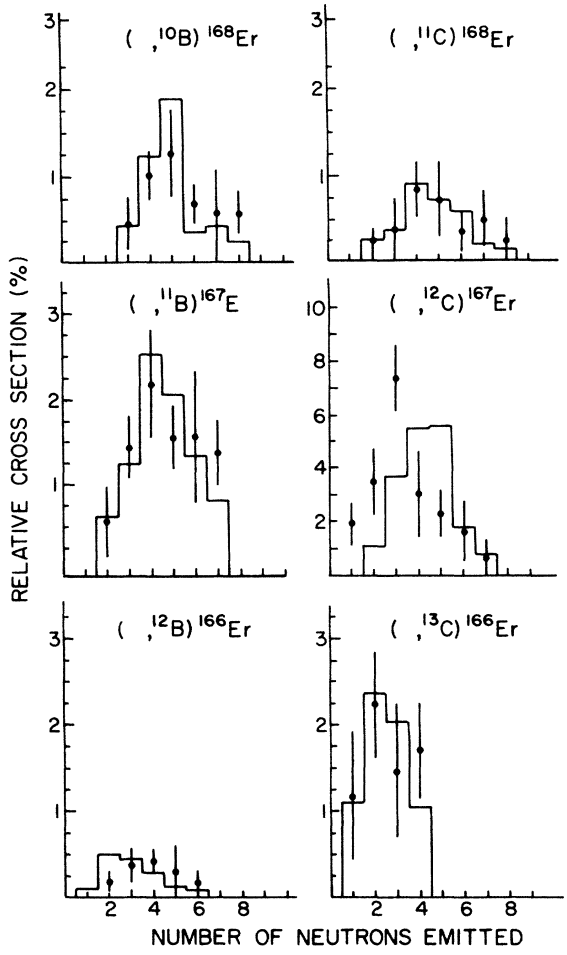

FIG. 9. Comparison of the observed isotropic distributions of TLF's (points) with a simple calculation (histograms); see the text. Each panel is labeled with the PLF and primary TLF. The experimental cross sections are presented in relative percentages of the inclusive PLF cross section. The calculations were normalized to the total area in each panel.

TABLE IV. TLF excitation energy distributions.

PLF	Absorbed fragment	Excitation energy range (MeV)	Angular momentum range ($\hbar$)
^{11}C	^{3}H	2.6–75.1	4–25
^{12}C	^{2}H	2.8–63.5	3–18
^{13}C	p	0.7–46.1	1–11
^{10}B	^{4}He	13.0–96.4	11–32
^{11}B	^{3}He	3.1–82.1	5–26
^{12}B	2p	0.6–57.7	2–17

good considering the simplicity of the assumptions. The average number and the range of evaporated neutrons are correctly predicted in four of the six cases. Only the centroids of the distributions calculated for fragmentation into mass 12 PLF's are different from the data by as much as two neutrons. Such differences may indicate the importance of sequential decay or other contributions to these PLF channels which are not present in the model calculations.

V. CONCLUDING REMARKS

We have reported the measurement of cross sections for the production of projectilelike fragments in coincidence with targetlike fragments at 20 MeV/nucleon. The cross sections were determined by the combination of isotopic identification of the light reaction products in a silicon surface barrier telescope and discrete line spectroscopy of the heavy residue. The complete identification of the reaction products was found to be limited to those transfer reactions with three or fewer nucleons by the broad isotopic distribution of TLF's associated with a given PLF. The fraction of the inclusive PLF cross section in coincidence with TLF γ rays is somewhat lower than the (20%–30%) obtained in a previous measurement of particle-γ-ray coincidences from ^{14}N-induced reactions with a rare earth target (^{159}Tb) at 10 MeV/nucleon,[4] as expected. However, both experiments (i.e., that of Ref. 4 and the present work) give fractions which are approximately a factor of 4 lower than the results from a recent PLF-charged particle coincidence measurement[17] for a similar system (^{20}Ne + ^{197}Au at comparable bombarding energies) for reasons that are not known.

The inclusive spectra of PLF's lighter than the projectile were compared to the Friedman and extended Serber breakup models. Both these calculations reproduce the spectral shape rather well. The energy spectra of PLF's resulting from the pickup reactions were well described in terms of direct transfer of a few nucleons from the target to the projectile. Finally, the isotropic distributions of TLF's were calculated by assuming that the unobserved fragment of the projectile was absorbed by the target which created an excited primary TLF that underwent statistical evaporation. These isotropic distributions agreed quite well with the observed TLF isotopic distributions.

ACKNOWLEDGMENTS

We would like to thank the staff of the National Superconducting Cyclotron Laboratory of Michigan State University for enabling us to perform the experiment. We would also like to thank S. M. Ferguson for his assistance in measuring the target impurities with the Western Michigan University tandem Van der Graaff accelerator. This work was supported by the National Science Foundation under Grant PHY-83-12245.

APPENDIX: ENERGY SPECTRA OF PLF'S RESULTING FROM PICKUP REACTIONS

In this appendix, we discuss the energy spectra of PLF's heavier than the projectile, which cannot be addressed in the framework of projectile breakup. These spectra (^{15}N, ^{15}O, and ^{16}O) show very sharp peaks compared to those of PLF's lighter than the projectile. An attempt was made to describe these data in terms of direct pickup of nucleon(s) from the target by the projectile. We write the longitudinal momentum distribution of the target nucleons, $\mathbf{P}_m$, by assuming that they are, on the average, at rest[18] with respect to the target by:

$$e^{-\mathbf{P}_m^2/2\sigma_1^2}, \tag{A1}$$

where m indicates the number of nucleons to be transferred and σ_1 is the width of the distribution which we estimated in a fashion similar to that of Friedman using a truncation radius parameter of 1.2 fm. Next we require linear momentum matching[19] in the longitudinal direction for the pickup process as:

$$e^{-(\mathbf{P}_m-\mathbf{P}_0)^2/2\sigma_2^2}, \tag{A2}$$

where $\mathbf{P}_0$ is the momentum of m nucleons at the beam velocity and σ_2 gives the width of the matching. Equation (A2) requires a soft landing of the "m" nucleons onto the projectile, i.e., an average relative velocity of zero. This is equivalent to the assumption used in the inverse (stripping) reaction that the "m" nucleons are at rest [$\lambda_1=0$ in equation (1) of Ref. 19] in the projectile frame. Equation (A2) thus ensures that only the higher momenta nucleons inside the target satisfy the matching condition. Neglecting recoil motion of the target for simplicity, the probability, w, of the pickup reaction is given by the product of Eqs. (A1) and (A2) and can be rewritten as:

$$w \propto e^{-(P_e-P_c)^2/2\sigma_r^2}. \tag{A3}$$

Now P_e is the local ejectile momentum and P_c is given by:

$$P_c=\frac{P_p+(P_p+P_0)u}{1+u} \tag{A4}$$

with the local projectile momentum P_p. By local we mean at the top of the Coulomb barrier. The reduced width, σ_r in Eq. (A3), is defined by:

$$\sigma_r^2=\sigma_1^2\sigma_2^2/(\sigma_1^2+\sigma_2^2)=\sigma_1^2/(1+u), \tag{A5}$$

where $u=\sigma_1^2/\sigma_2^2$. In writing Eq. (A3), we use the relation

$P_e = P_m + P_p$, assuming that the transfer of "m" nucleons takes place in the reaction plane. The energy spectra of the ejectile is then given by:

$$d^2\sigma/dE\,d\Omega \propto \rho_e \rho_r w \ , \tag{A6}$$

where $\rho_e \propto A_e E_e^{1/2}$ and $\rho_r \propto (A_t - A_m)(280 + Q_{\text{eff}} - E_e)^{1/2}$ are the ejectile and the residue phase space factors, respectively. A_i ($i = e$, t, or m) is the mass number of i, E_e is the ejectile energy, and Q_{eff} is the effective Q value which is the sum of the reaction Q value and the Coulomb energy difference between the entrance and exit channels. The phase space ρ_r results in a sharp cutoff seen on the high energy side of the spectra.

The width σ_1 of the intrinsic momentum distribution in a ^{165}Ho nucleus is calculated to be 48 MeV/c for a neutron, 45 MeV/c for a proton, and 60 MeV/c for a deuteron. We treated σ_2 as a free parameter and determined the value so as to reproduce the experimental most probable kinetic energy. The value of σ_2 was found to be 74 MeV/c for ^{15}N, 80 MeV/c for ^{15}O, and 86 MeV/c for ^{16}O. The spectra calculated with Eq. (A6) are shown by the dotted-dashed lines in Fig. 2.

An alternative estimation of σ_2 could be made by applying Friedman's breakup model to the inverse process of the pickup, i.e., in the time-reversed reaction ^{15}N fragments into ^{14}N plus a neutron. Using a truncation radius parameter of 1.2 fm, we obtain similar values for σ_2 of 84 MeV/c for ^{15}N, 78 MeV/c for ^{15}O, and 106 MeV/c for ^{16}O. The kinetic energy spectra obtained with this model are shown by the dotted curves in the figure. The overall agreement of both calculations with the data is satisfactory, particularly in view of the simplicity of the assumptions.

---

*Permanent address: Cyclotron Institute, Texas A&M University, College Station, TX 77843.

†Permanent address: Department of Physics, Alma College, Alma, MI 48801.

‡On leave from Institute of Experimental Physics, University of Warsaw, 00-681, Warsaw, Poland. Present address: Lawrence Berkeley Laboratory, Nuclear Physics Division, Berkeley, CA 94720.

§On leave from Institute for Nuclear Studies, 05-400 Swierk (Warsaw), Poland. Present address: Lawrence Berkeley Laboratory, Nuclear Physics Division, Berkeley, CA 94720.

[1]T. Inamura, M. Ishihara, T. Fukuda, T. Shimoda, and H. Hiruta, Phys. Lett. **68B**, 51 (1977).

[2]D. R. Zolnowski, H. Yamada, S. E. Cala, A. C. Kahler, and T. T. Sugihara, Phys. Rev. Lett. **41**, 92 (1978).

[3]K. Siwek-Wilczynska, E. H. du Marchie van Voorthuysen, J. van Popta, R. H. Siemssen, and J. Wilczynski, Phys. Rev. Lett. **42**, 1599 (1979).

[4]J. Wilczynski, K. Siwek-Wilczynska, J. van Driel, S. Gonggrijp, D. C. J. M. Hageman, R. V. F. Janssens, J. Lukasiak, R. H. Siemssen, and S. Y. van der Werf, Nucl. Phys. **A373**, 109 (1982).

[5]K. Bhowmik, J. van Driel, R. H. Siemssen, G. J. Balster, P. B. Goldhoorn, S. Gonggrijp, Y. Iwasaki, R. V. F. Janssens, H. Sakai, K. Siwek-Wilczynska, W. A. Sterrenberg, and J. Wilczynski, Nucl. Phys. **A390**, 117 (1982).

[6]T. Udagawa, D. Price, and T. Tamura, Phys. Lett. **118B**, 45 (1982); T. Udagawa and T. Tamura, Phys. Rev. C **24**, 1348 (1981).

[7]J. van Driel, S. Gonggrijp, R. V. F. Janssens, R. H. Siemssen, K. Siwek-Wilczynska, and J. Wilczynski, Phys. Lett. **98B**, 351 (1981).

[8]H. Utsunomiya, Phys. Rev. C **32**, 849 (1985).

[9]W. A. Friedman, Phys. Rev. C **27**, 569 (1983).

[10]H. Utsunomiya, D. J. Morrissey, R. A. Blue, L. H. Harwood, R. M. Ronningen, K. Siwek-Wilczynska, and J. Wilczynski, in Proceedings of the 1984 INS-RIKEN International Symposium of Heavy Ion Physics, Mt. Fuji, Japan, edited by S. Kubono, M. Ishihara, and M. Ichimura, J. Phys. Soc. Jpn. **54**, Suppl. II, 63 (1985).

[11]K. Siwek-Wilczynska, R. A. Blue, L. H. Harwood, R. M. Ronningen, H. Utsunomiya, J. Wilczynski, and D. J. Morrissey, Phys. Rev. C **32**, 1450 (1985).

[12]L. Westerberg, D. G. Sarantites, R. Lovett, J. T. Hood, J. H. Barker, C. M. Currie, and N. Mullani, Nucl. Instrum. Methods **145**, 295 (1977).

[13]*Table of Isotopes*, edited by C. M. Lederer and V. S. Shirley, 7th ed. (Wiley, New York, 1978), and references therein.

[14]N. Matsuoka, A. Simizu, K. Hosono, T. Saito, M. Kondo, H. Sakaguchi, Y. Toba, A. Goto, F. Ohtani, and N. Nakanishi, Nucl. Phys. **A311**, 173 (1978).

[15]C. K. Gelbke, D. K. Scott, M. Bini, D. L. Hendrie, J. L. Laville, J. Mahoney, M. C. Mermaz, and C. Olmer, Phys. Lett. **70B**, 415 (1977).

[16]F. Piasil, Oak Ridge National Laboratory Report ORNL-TM-6054, 1977 (unpublished).

[17]R. G. Stokstad, C. R. Albiston, M. Bantel, Y. Chan, P. J. Countryman, S. B. Gazes, B. G. Harvey, H. Homeyer, M. J. Murphy, I. Tserruya, K. van Bibber, and S. Wald, Proceedings of the 1984 INS-RIKEN International Symposium on Heavy Ion Physics, Mt. Fuji, Japan, edited by S. Kubono, M. Ishihara, and M. Ichimura, J. Phys. Soc. Jpn. **54**, Suppl. II, 71 (1985); S. Wald, S. B. Gazes, C. R. Albiston, Y. Chan, B. G. Harvey, M. J. Murphy, I. Tserruya, R. G. Stokstad, P. J. Countryman, K. Van Bibber, and H. Homeyer, Phys. Rev. C **32**, 894 (1985).

[18]P. J. Siemens, J. P. Bondorf, D. H. E. Gross, and F. Dickmann, Phys. Lett. **36B**, 24 (1971).

[19]D. M. Brink, Phys. Lett. **40B**, 37 (1972).